Assessment of cardiac time intervals using high temporal resolution real-time spiral phase contrast with UNFOLDed-SENSE

Grzegorz T Kowalik, Daniel S Knight, Jennifer A Steeden, Oliver Tann, Freddy Odille, David Atkinson, Andrew Taylor, Vivek Muthurangu

PRECLINICAL AND CLINICAL IMAGING – Note

Magnetic Resonance in Medicine 73:749–756 (2015)

Assessment of Cardiac Time Intervals Using High Temporal Resolution Real-Time Spiral Phase Contrast with UNFOLDed-SENSE

Grzegorz T. Kowalik,[1] Daniel S. Knight,[1,2] Jennifer A. Steeden,[1] Oliver Tann,[1,3] Freddy Odille,[4,5] David Atkinson,[6] Andrew Taylor,[1,3] and Vivek Muthurangu[1,3]*

Purpose: To develop a real-time phase contrast MR sequence with high enough temporal resolution to assess cardiac time intervals.

Methods: The sequence utilized spiral trajectories with an acquisition strategy that allowed a combination of temporal encoding (Unaliasing by fourier-encoding the overlaps using the temporal dimension; UNFOLD) and parallel imaging (Sensitivity encoding; SENSE) to be used (UNFOLDed-SENSE). An in silico experiment was performed to determine the optimum UNFOLD filter. In vitro experiments were carried out to validate the accuracy of time intervals calculation and peak mean velocity quantification. In addition, 15 healthy volunteers were imaged with the new sequence, and cardiac time intervals were compared to reference standard Doppler echocardiography measures. For comparison, in silico, in vitro, and in vivo experiments were also carried out using sliding window reconstructions.

Results: The in vitro experiments demonstrated good agreement between real-time spiral UNFOLDed-SENSE phase contrast MR and the reference standard measurements of velocity and time intervals. The protocol was successfully performed in all volunteers. Subsequent measurement of time intervals produced values in keeping with literature values and good agreement with the gold standard echocardiography. Importantly, the proposed UNFOLDed-SENSE sequence outperformed the sliding window reconstructions.

Conclusion: Cardiac time intervals can be successfully assessed with UNFOLDed-SENSE real-time spiral phase contrast. Real-time MR assessment of cardiac time intervals may be beneficial in assessment of patients with cardiac conditions such as diastolic dysfunction. **Magn Reson Med 73:749–756, 2015.** © **2014 Wiley Periodicals, Inc.**

Key words: UNFOLD; real-time spiral PC-MR; cardiac timing intervals

INTRODUCTION

Cardiac time intervals (e.g., isovolumic times and ejection time) can provide important information about integrated myocardial function (1). Usually time intervals are assessed by Doppler echocardiographic measurement of ventricular inflow and outflow patterns, but they could also be assessed with velocity-encoded phase-contrast MR (PC-MR). However, PC-MR is conventionally cardiac-gated, and this introduces two major problems. First, flow patterns produced by gated PC-MR may be distorted by interbeat variation in stroke volume and heart rate. This has little effect on quantification of velocity, but may affect the reliability of time interval measurement. Second, acquiring gated data with sufficiently high temporal resolution takes several minutes, limiting its utility in the clinical environment. An alternative approach is accelerated real-time PC-MR with very high temporal resolution. Two commonly used methods of accelerating real-time imaging are: efficient k-space filling (e.g., echo-planar or spiral trajectories) and parallel imaging techniques (e.g., sensitivity encoding [SENSE]) (2). Unfortunately, even when combined these techniques do not provide the necessary temporal resolution to accurately measure time intervals.

Previously, k-t broad-use linear acquisition speed-up technique (BLAST) or k-t SENSE (3) methods have been used to achieve higher acceleration factors for Cartesian and radial real-time imaging (4). However, when using spiral trajectories the requirement for training data necessitates the use of variable density spirals, reducing the achievable acceleration and increasing imaging artefacts due to longer readouts). A better approach for spiral imaging may be the unaliasing by Fourier-encoding the overlaps using the temporal dimension (UNFOLD) technique (5). In UNFOLD, an alternating undersampling pattern results in aliasing in the temporal frequency (f) domain being displaced to the Nyquist frequency. As the aliasing

[1]UCL Institute of Cardiovascular Science, Centre for Cardiovascular Imaging, London, United Kingdom.

[2]Division of Medicine, University College London, Royal Free Campus, Rowland Hill Street, London, United Kingdom.

[3]Cardiorespiratory Unit, Great Ormond Street Hospital for Children, London, United Kingdom.

[4]IADI, INSERM U947, Nancy, France.

[5]Université de Lorraine, Nancy, France.

[6]Centre for Medical Imaging, UCL Division of Medicine, London, United Kingdom.

Grant sponsor: GTK funded by Siemens Medical Systems; DSK funded by British Heart Foundation; JAS funded by British Heart Foundation; AT funded by the National Institute for Health Research; and VM funded by British Heart Foundation. The work was carried out with support of the GOSH/ ICH NIHR Biomedical Research Centre.

*Correspondence to: Vivek Muthurangu, MD, Cardiorespiratory Unit, 6th Floor, Nurses Home, Great Ormond Street Hospital for Children, Great Ormond Street, London, WC1N 3JH, UK. E-mail: v.muthurangu@ucl.ac.uk

Additional Supporting Information may be found in the online version of this article.

Received 4 September 2013; revised 21 January 2014; accepted 26 January 2014

DOI 10.1002/mrm.25183

Published online 14 February 2014 in Wiley Online Library (wileyonlinelibrary.com).

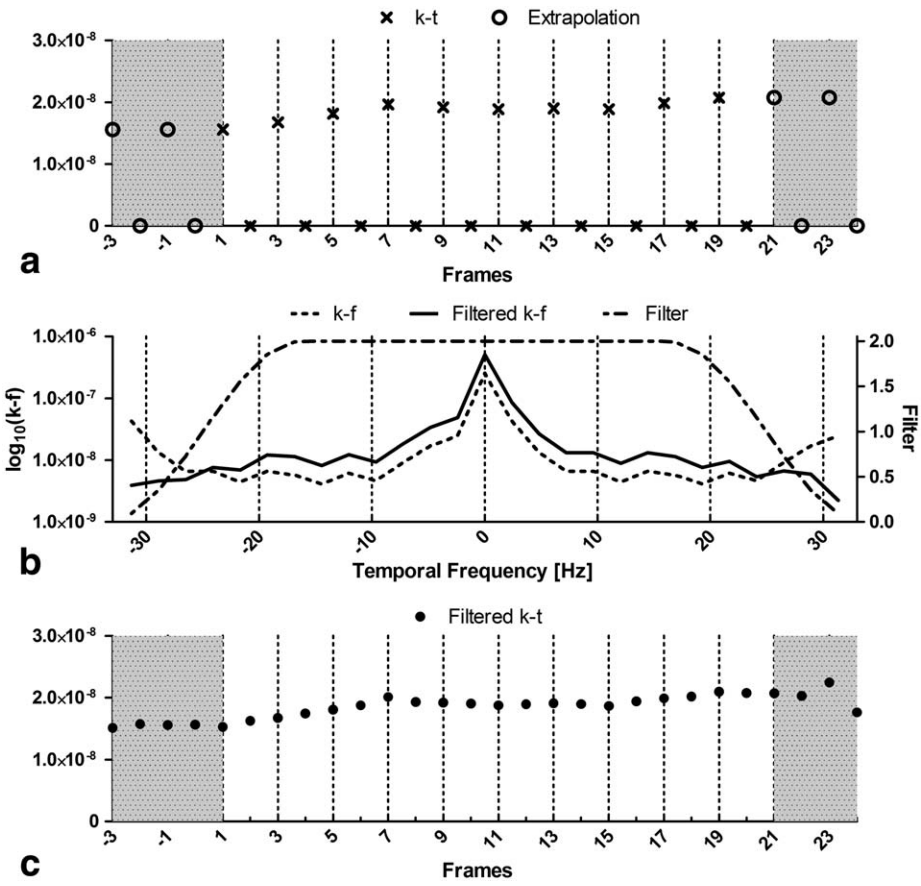

FIG. 1. Schematic visualisation of the temporal filtering used in the UNFOLDed-SENSE reconstruction: **(a)** plot of the magnitude of a k-space sample through time (note the two-fold undersampling); **(b)** temporal frequency of the sample before and after filtering; and **(c)** plot of the magnitude of a k-space sample through time after UNFOLD filtering (note that the data is now fully sampled through time). Grey area indicates extrapolated data, which were discarded after the UNFOLD to suppress possible ringing artefact.

can be removed using a simple low-pass filter, no training data is required; therefore, it can easily be combined with uniform density spirals. Combining UNFOLD, spiral trajectories (5,6), and SENSE (2,7,8) should allow the acquisition of real-time data with high enough temporal resolution to assess cardiac time intervals.

In this study, a high temporal resolution, real-time spiral PC-MR sequence that combined UNFOLD and SENSE reconstructions (UNFOLDed-SENSE) was implemented. The purpose of this study was to validate the measurement of time intervals using this sequence in silico, in vitro, and in vivo.

METHODS

MR Protocol

All imaging was performed on a 1.5 Tesla MR scanner (Avanto, Siemens Medical Solutions, Erlangen, Germany) using six-element spine and body matrix coils (total of 12 elements used for acquisition).

Real-time PC-MR Sequence

Acquisition

Real-time PC-MR was performed using a uniform density spiral sequence (9). The imaging parameters were: Field of view (FOV), 450 × 450 mm; matrix, 128 × 128; voxel size, 3.5 × 3.5 × 7 mm; repetition time (TR)/echo time (TE), 7.41/1.97 ms; flip angle, 20°; velocity encoding (VENC), 150 cm/s; and complete k-space sampling, 10 interleaves. In order to minimize TR, neither water-only excitation nor fat-suppression pulses were used.

To achieve high temporal resolution (<15 ms), one interleave was acquired per frame, and the resulting 10× undersampled data was reconstructed using UNFOLDed-SENSE. A novel acquisition scheme was implemented to fulfill both the UNFOLD criteria and a self-referencing SENSE approach for the calculation of coil sensitivity maps (7). The UNFOLD criteria were met by acquiring alternate lines in consecutive frames, while full sampling of k-space was enabled by rotating this pair of alternating lines every 20 frames. This allowed maps to be calculated by combining data from 100 frames, with the resultant maps having 10 signal averages (Supporting Fig. 1). This data acquisition scheme required the total number of frames to be a multiple of 100. In this study, 700 frames were acquired in ≈10.37 s.

Reconstruction

All real-time UNFOLDed-SENSE reconstructions were performed "online" using a graphical processing unit (GPU) (Tesla C2070, Nvidia, Santa Clara, CA, USA)-equipped external computer that was networked to the native scanner reconstruction system (10). In our implementation, UNFOLD was performed before the SENSE reconstruction.

UNFOLD was performed separately on consecutive sets of 20 k-space frames in which the same alternating

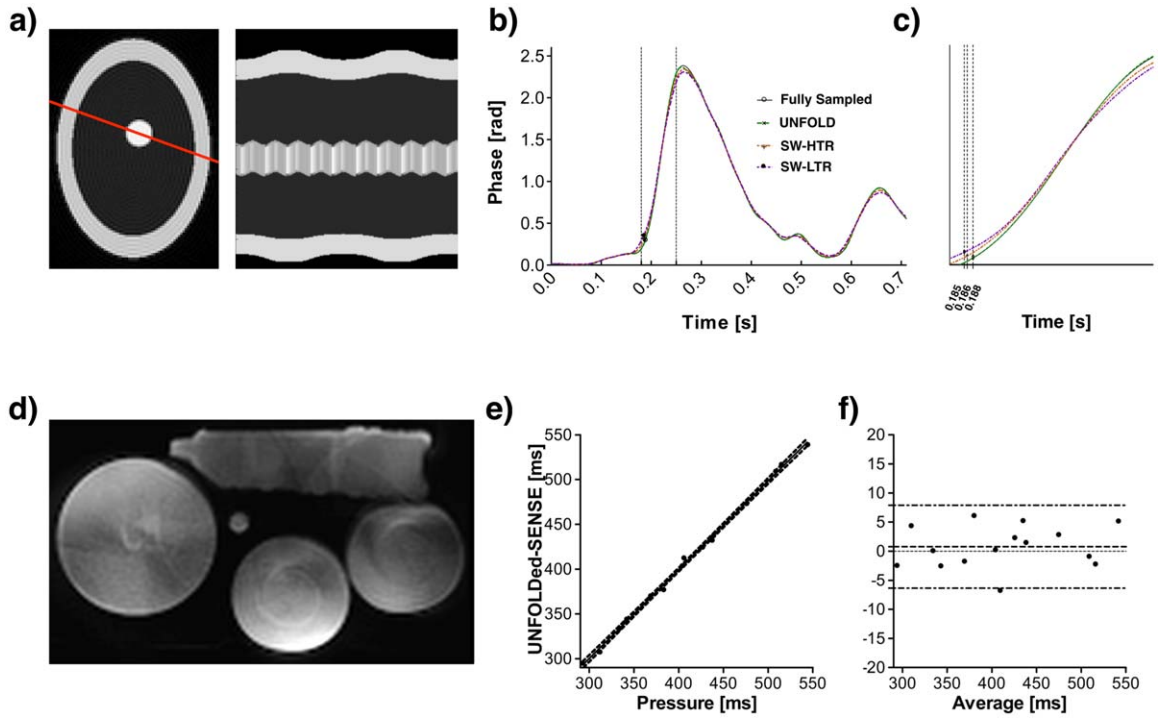

FIG. 2. In silico and in vitro results: **(a)** Visual representation of the in silico model, including a cross-section (shown by red line) time representation to display motion. **(b)** The average phase curves extracted from simulated mitral valve orifice for all real-time reconstructions. **(c)** Closeup of the ascending slope of the simulated E wave showing displacement of its starting point at 0.188 s (calculated as the x-intercept of a tangent line through the inflection point) in the SW-HTR (0.186 s) and SW-LTR reconstructions (0.185 s) due to temporal blurring. (**d)** In vitro phantom reconstructed with the UNFOLDed-SENSE reconstruction. The phantom consisted of three doped water bottles, a bottle of oil, and a nondistensible polyvinyl chloride (PVC) pipe placed in middle. **(e)** Bland–Altman and scatter plots of UNFOLDed-SENSE measured time intervals against the reference standard pressure measurements.

interleaves were acquired. Within each group, each k-space position in an acquired interleave was 2× undersampled in time (Fig. 1). Thus, Fourier transformation along time resulted in aliasing at the Nyquist temporal frequency. The aliases were removed using a low-pass temporal frequency filter. After inverse Fourier transformation, every k-space position in an acquired interleave was fully sampled in time (Fig. 1). This resulted in each k-space frame containing two interleaves, a reduction in undersampling from 10× to 5×. The optimum filter characteristics were chosen using an in silico experiment, as described below. In addition, prior to UNFOLD each set of 20 frames was extended by four frames in either direction (by replicating the first and last 2 frames). Ringing introduced by the filtering process was "pushed" into these additional frames, which were then discarded prior to SENSE reconstruction (11).

Coil sensitivity maps were calculated by combining the velocity compensated interleaves from 100 consecutive frames (the minimum number of frames required to ensure complete k-space filling). These coil sensitivity maps were used in the iterative non-Cartesian SENSE reconstruction on the same 100 frames after they have undergone the UNFOLD reconstruction.

Two additional two-frame sliding window reconstructions were also carried out on the acquired data. As the UNFOLDed-SENSE, both sliding windows reconstructions reduced the acceleration from 10× to 5× and required SENSE reconstruction prior to visualization. The first reconstruction used an overlapping sliding window and had the same frame rate as the UNFOLDed-SENSE reconstruction (SW-HTR). The second reconstruction used a nonoverlapping sliding window; consequently, the reconstructed data had half the frame rate of the raw data (SW-LTR).

In Silico Simulation

The in silico model consisted of a high-intensity border representing subcutaneous fat, plus an internal medium-intensity ellipse representing the ventricular short axis at the mitral valve level (Fig. 2a). Respiratory motion (Fig. 2a) was modelled using a function consisting of expansion (inhalation), a brief pause, and contraction (exhalation). The respiratory rate was ≈0.22 Hz, with the outer border increasing by ≈11% of its original size. Cardiac motion (Fig. 2a) was simulated by sinusoidaly, translating the internal ellipse along a diagonal trajectory. The simulated heart rate was ≈1 Hz, and the amplitude of translation was of ≈30% of the internal ellipse size. Blood flow velocity at the mitral valve orifice was modelled on a real mitral valve inflow (MVI) trace acquired using high temporal-resolution Doppler echocardiography (SC2000 cardiac ultrasound system, Siemens Healthcare, Erlangen, Germany) (pulsed-wave Doppler frequency 1.75 MHz; sweep speed: 100–150 mm/s) with a peak phase of 0.9 Π rad.

Simulated MR data was created by downsampling the model data to a temporal resolution of ≈14.8 ms and extracting k-space data on 10 spiral interleaves with a matrix of 128 × 128 points. We choose not to simulate the total undersampling in our sequence because the in silico model was only created to select the optimum UNFOLD filter. Therefore, each simulated k-space frame was undersampled by a factor of 2 in an alternating manner to simulate the 2× temporal undersampling in our sequence. The benefit of reducing the acceleration in this model was that it was not necessary to simulate the SENSE reconstruction, which may have led to suboptimal filter choice due to imperfections of coil sensitivity simulations. The undersampled k-space data underwent the UNFOLD reconstruction with different Tukey filters. Two filter characteristics were varied: i) the passband (20%–100% of temporal frequency, in increments of 5%) and ii) the position of the stopband corners (passband edge–Nyquist frequency; in increments of 5%). The resultant data was gridded, and Fourier was transformed into image space. The average phase in the simulated mitral valve orifice for each filter was compared to the fully sampled data (reconstructed by gridding and inverse Fourier transformation). The optimal filter was the one with the lowest normalized root-mean-square error (NRMSE). The temporally undersampled data also underwent both sliding window reconstructions for comparison (Fig. 2b, c).

In Vitro Validation

The in vitro phantom consisted of a polyvinyl chloride (PVC) pipe (length: ≈12.5 m; internal diameter: 0.2 m) surrounded by water and oil bottles (width 400 mm; height 200 mm) (Fig. 2d). Fifteen experiments were performed with different stroke volumes (range: 25–45 ml) and heart rates (range: 60–130 beats per min) using a pulsatile flow pump (Harvard Apparatus, Holliston, MA, USA). These values were chosen to produce peak mean velocities and ejection times in the normal range seen in humans. Ejection times were compared to simultaneously acquired pressure curves (the reference standard) measured at the same position as the imaging planes using MR-compatible pressure transducers (Datex-Ohmeda, GE Healthcare, Helsinki, Finland) with 1 kHz sampling frequency. Peak mean velocities measured using the three real-time reconstructions were compared to the reference standard Cartesian PC-MR sequence (FOV: 400 × 300 mm; matrix: 192 × 144; voxel size: 2.1 × 2.1 × 5 mm; TR/TE: 10.7/2.5 ms; temporal resolution: ≈10.7 ms; flip angle: 20°). The peak mean velocity and ejection time of the flow curve produced by the pump was analyzed in the same way as described below.

In Vivo Study

Study Population

Fifteen healthy volunteers (6 male and 9 female) were recruited for this study between April and May 2013. The median age was 43 (range 27–66 years). Exclusion criteria were: i) Cardiovascular disease (assessed by clinical history); ii) contraindications to MR; and iii) cardiac rhythm abnormalities, including heart block. The local research ethics committee approved the study, and written consent was obtained from all volunteers.

Imaging Protocol

A plane at the base of the heart was selected so that both the MVI and left ventricular outflow tract (LVOT) were imaged in the short axis (Fig. 3). Flow data in this plane were collected using the real-time UNFOLDed-SENSE PC-MR, which was also reconstructed using the sliding window reconstructions, and a high-resolution Cartesian gated scan (same parameters as for the in vitro study). Transthoracic echocardiography was performed immediately prior to or after the MR examination (same system as for the in silico experiment). Pulsed-wave Doppler recordings were acquired separately in the LVOT (apical five-chamber view) and at the MVI in the apical four-chamber view.

Image Analysis

All PC-MR data (in vitro and in vivo) were segmented using a registration-based algorithm (12) with manual user correction (OsiriX Foundation, Geneva, Switzerland) (13). Velocity curves were sinc interpolated to ≈1 ms temporal resolution. MVI mean velocity curves contained early (E wave) and late diastolic waves (A wave), whereas LVOT velocity curves contained systolic ejection wave (S wave). The start and end of each wave were automatically defined by tangent lines calculated at the inflection points of ascending and descending slopes of the wave. Ejection time (ET), isovolumic contraction time (ICT), and isovolumic relaxation time (IRT) were calculated as shown in Figure 3. Tei index is defined as (IRT + ICT)/ET. The E/A ratio was the ratio between the peak of the mean E and A wave velocity curves. Doppler echocardiographic data were manually processed, and time intervals were calculated as previously described using both the LVOT and MVI Doppler traces and the concurrently acquired ECG (14).

Estimation of signal-to-noise ratio (SNR) and velocity-to-noise ratio (VNR) in the in vivo data was performed as previously described (15,16). A region-of-interest (ROI) was drawn in stationary tissue, and estimated noise was calculated as the average standard deviation of the pixel intensity or velocity through all time frames. Final estimates of SNR were made from the mean signal intensity, and VNR from the mean velocity within a ROI was drawn in the vessel during peak systole and divided by their noise estimates.

Statistical Analysis

Results of in silico tests were compared using NRMSE metric normalized with respect to the reference data. This allowed for a direct comparison and selection of the optimal filter. For real-time data, each cardiac cycle was analyzed separately and then averaged to produce the final result, which was compared to the Cartesian gated PC-MR both in vivo and in vitro. Time intervals, peak mean velocities, SNR, and VNR were expressed as mean ± standard deviation. Measurements of agreement

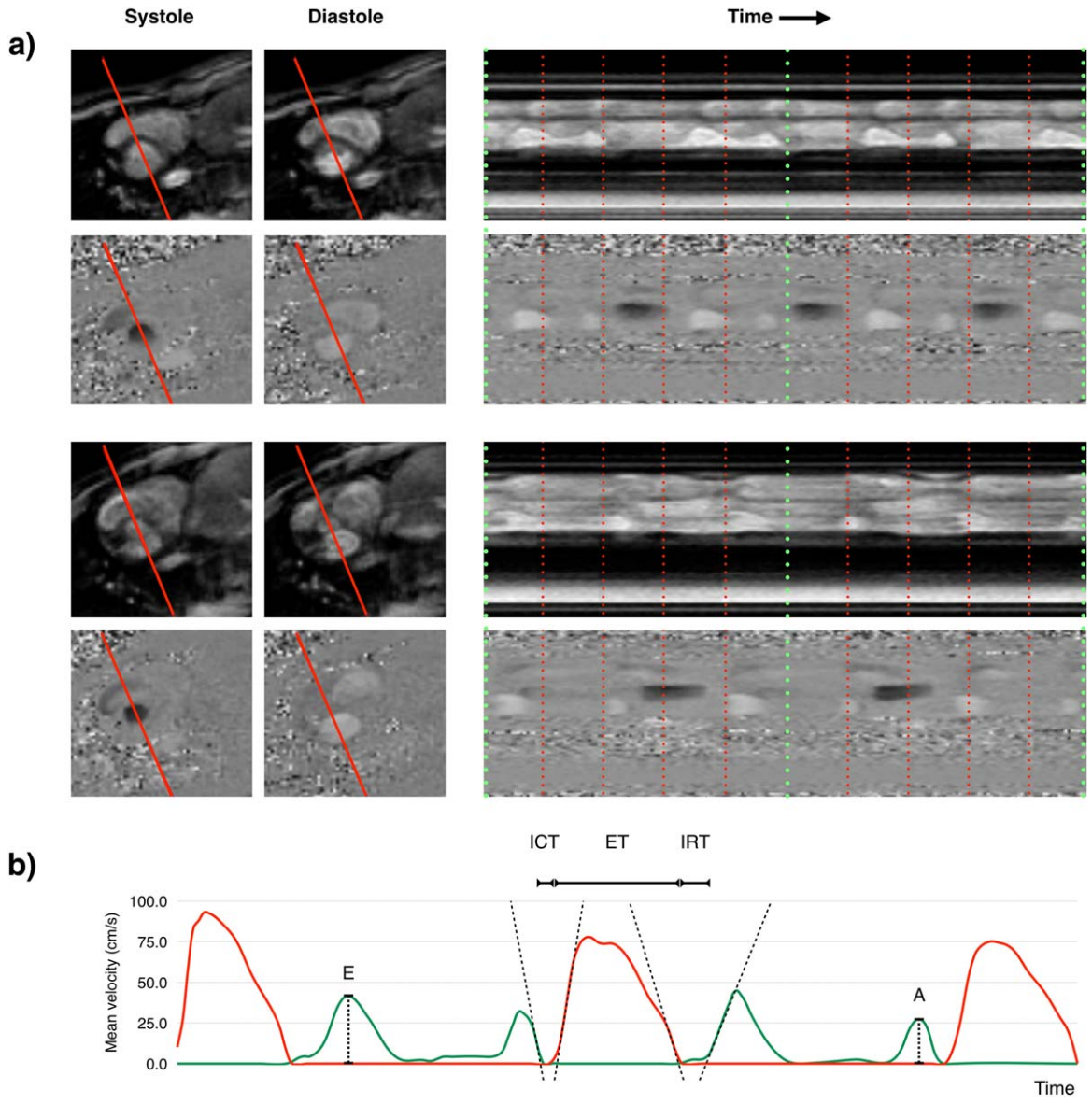

FIG. 3. **(a)** Examples from two volunteers of magnitude and phase images reconstructed with the UNFOLDed-SENSE reconstruction, at systole, diastole, and represented as a cross section (as shown by red line) against time image. The red dotted lines represent transitions between 20 frame blocks that underwent UNFOLD; and the green dotted lines represent the transition between 100 frame blocks that underwent SENSE. **(b)** Plot of left ventricular outflow tract (red line) and mitral valve inflow (green line) velocity curves. The start and end of the S wave, the start of the E wave, and the end of the A wave are delineated by the horizontal axis intercepts of tangent lines drawn on the ascending and descending slopes of the respective waves. These are then used to calculate: isovolumic relaxation time (IRT), isovolumic contraction time (ICT), and ejection time (ET), as shown.

were performed using Bland–Altman, and correlation analysis and differences between means was tested using ANOVA with post hoc Bonferroni testing.

RESULTS

In Silico Tests

The optimal UNFOLD filter had a passband of 48% and stopband corners at the Nyquist frequency ≈33.7 Hz (−3 dB cutoff frequency at ≈25 Hz, resulting in ≈20 ms temporal resolution). The NRMSE of the optimal UNFOLD filter was 0.33%, compared to the SW-HTR NRMSE of 0.66% and SW-LFR NRMSE of 1.22%. Figure 2b–2c shows the velocity curves generated by the three reconstructions, with the SW-HTR and SW-LTR curves exhibiting temporal blurring that affected their ability to accurately reproduce the starting point of the simulated E wave.

In Vitro Validation

The results for in vitro experiments are shown in Table 1 and Figure 2. The ejection times calculated using the UNFOLDed-SENSE and SW-HTR data were similar to reference standard pressure measurement, with negligible biases, narrow limits of agreement, and excellent correlations. Both the SW-LFR and the gated Cartesian data

Table 1
Combined In Vitro and In Vivo Results of Bland–Altman and Correlation Analyses

Mean Velocity	Mean (cm/s)	Bias (cm/s)	Limits (cm/s)	Correlation
Cartesian gated	40.86 ± 9.07	–	–	–
UNFOLDed-SENSE	40.73 ± 8.96	−0.13 ± 0.84	−1.79 : 1.52	r = 0.996
SW-HTR	40.44 ± 8.78	−0.42 ± 0.89	−2.16 : 1.32	r = 0.996
SW-LTR	40.37 ± 8.51	−0.49 ± 1.46	−3.34 : 2.36	r = 0.988

Time Intervals	Mean (ms)	Bias (ms)	Limits (ms)	Correlation
Pressure curves	412.59 ± 73.55	–	–	–
Cartesian gated[b]	404.94 ± 68.22	7.65 ± 11.15[a]	−14.22 : 29.51	r = 0.990
UNFOLDed-SENSE	411.83 ± 72.98	0.76 ± 3.51	−6.12 : 7.64	r = 0.999
SW-HTR	411.90 ± 74.39	0.69 ± 6.83	−12.69 : 14.08	r = 0.996
SW-LTR	410.24 ± 69.07	2.35 ± 10.58	−18.38 : 23.09	r = 0.991

ICT	Mean (ms)	Bias (ms)	Limits (ms)	Correlation
Echo	46.42 ± 12.64	–	–	–
Cartesian gated[b]	39.58 ± 12.28	−6.84 ± 8.96 [a]	−24.39 : 10.71	r = 0.759
UNFOLDed-SENSE	45.02 ± 11.57	−1.40 ± 5.55	−12.67 : 9.87	r = 0.898
SW-HTR	42.45 ± 11.63	−3.97 ± 6.94[a]	−17.58 : 9.63	r = 0.850
SW-LTR	41.82 ± 13.24	−4.60 ± 8.62	−21.49 : 12.29	r = 0.794

IRT	Mean (ms)	Bias (ms)	Limits (ms)	Correlation
Echo	73.80 ± 14.71	–	–	–
Cartesian gated[b]	56.73 ± 12.54	−17.06 ± 13.76[a]	−44.03 : 9.09	r = 0.534
UNFOLDed-SENSE	74.13 ± 9.26	0.33 ± 9.61	−18.51 : 19.17	r = 0.793
SW-HTR	71.53 ± 9.33	−2.26 ± 10.58	−23.00 : 18.47	r = 0.724
SW-LTR	70.48 ± 9.20	−3.32 ± 11.44	−25.74 : 19.11	r = 0.661

Ejection Time	Mean (ms)	Bias (ms)	Limits (ms)	Correlation
Echo	301.09 ± 21.43	–	–	–
Cartesian gated[b]	310.33 ± 20.89	9.24 ± 17.81	−25.67 : 44.16	r = 0.669
UNFOLDed-SENSE	305.99 ± 19.02	4.90 ± 11.73	−18.10 : 27.90	r = 0.849
SW-HTR	308.07 ± 19.13	6.98 ± 10.77[a]	−14.12 : 28.08	r = 0.875
SW-LTR[b]	309.49 ± 19.24	8.40 ± 11.35[a]	−13.86 : 30.65	r = 0.860

Tei	Mean	Bias	Limits	Correlation
Echo	0.40 ± 0.06	–	–	–
Cartesian gated[b]	0.31 ± 0.05	−0.088 ± 0.069[a]	−0.226 : 0.047	r = 0.378[a]
UNFOLDed-SENSE	0.39 ± 0.04	−0.010 ± 0.046	−0.099 : 0.080	r = 0.721
SW-HTR	0.37 ± 0.05	−0.029 ± 0.053	−0.133 : 0.075	r = 0.610
SW-LTR[b]	0.36 ± 0.05	−0.036 ± 0.058[a]	−0.150 : 0.077	r = 0.523

E/A	Mean	Bias	Limits	Correlation
Echo	1.42 ± 0.29	–	–	–
Cartesian gated	1.47 ± 0.35	0.047 ± 0.245	−0.433 : 0.528	r = 0.745
UNFOLDed-SENSE	1.55 ± 0.39	0.128 ± 0.288	−0.435 : 0.692	r = 0.698
SW-HTR[b]	1.57 ± 0.38	0.145 ± 0.283	−0.410 : 0.699	r = 0.697
SW-LTR	1.55 ± 0.39	0.127 ± 0.299	−0.459 : 0.713	r = 0.681

[a]Fixed bias or insignificant correlation (95% confidence).
[b]Significant difference in Bonferroni's Multiple Comparison test (95% confidence) against the reference standard measurement.

overestimated the ejection time (positive bias) with wider limits of agreement and poorer correlation. Peak mean velocities from three real-time reconstructions agreed well with the reference standard gated Cartesian PC-MR sequence. Nevertheless, UNFOLDed-SENSE performed marginally better. A residual spiral artefact can be seen on the phantom image (Fig. 2d), possibly due to suboptimal distribution of receiver coils. These spatial artefacts seemed to have no or very little effect on quantitative assessment of flow or time intervals.

In Vivo Study

The results are presented in Table 1 and Figure 3. There was good agreement for all time intervals (including Tei index) between UNFOLDed-SENSE data and Doppler

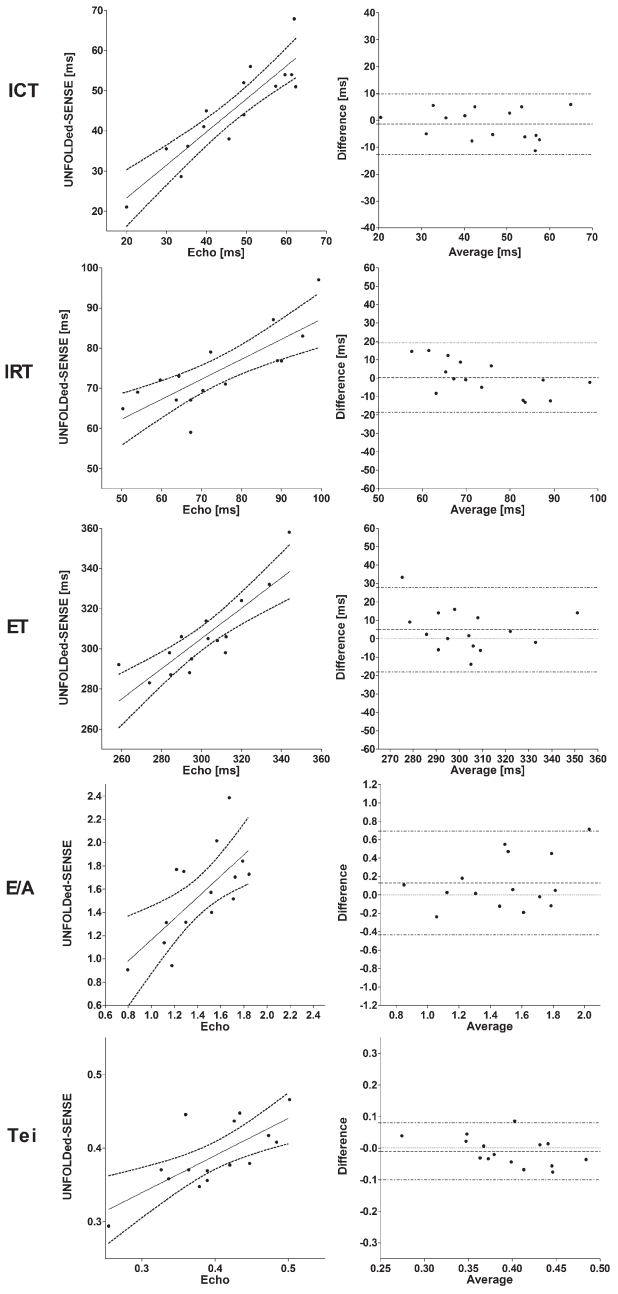

FIG. 4. Bland-Altman and scatter plots of the UNFOLDed-SENSE against Doppler echocardiography. All of the measured ventricular function parameters had a good agreement with all negligible biases and acceptable limits of agreement, as well as strong correlations.

echocardiography, with negligible biases, reasonable limits of agreement, and good correlations (Fig. 4). The SW-LFR and SW-HTR reconstructions performed less well, with increasing biases and generally wider limits of agreement. Cartesian PC-MR performed worst of all, with clinically significant biases, wide limits of agreement, and poor correlation compared to echocardiography. For assessment of E/A ratio, all of the real-time reconstruction performed reasonably well, with similar biases, limits of agreement and correlations. However, Cartesian PC-MR performed best, with negligible bias, narrower limits of agreement, and better correlation.

There was no statistically significant ($P > 0.6$) difference between the UNFOLDed-SENSE, SW-HTR, or SW-LTR reconstructions in terms of SNR (27.4 ± 7.3, 26.8 ± 8.4, and 28.5 ± 7.6, respectively) or VNR (21.7 ± 5.7, 23.9 ± 6.5, and 23.2 ± 6.0, respectively). SNR and VNR were highest for the Cartesian gated sequence (40.4 ± 8.5 and 32.0 ± 11.8, respectively) and were significantly different from the real-time reconstructions ($P < 0.05$).

DISCUSSION

We have shown that it is possible to accurately measure cardiac time intervals using real-time UNFOLDed-SENSE PC-MR, and that this approach is superior to gated PC-MR. This superiority is probably due to the differential affects of interbeat heart rate and stroke volume variability. Gated PC-MR data is produced by averaging over multiple heartbeats; consequently, interbeat variability results in the temporal blurring of flow data and errors during processing. In real-time PC-MR, each heartbeat is processed separately; therefore, the raw measurements are unaffected by interbeat variability. Although these raw measurements are averaged, the strong agreement with Doppler suggests that averaging processed data does not lead to the same inaccuracies as processing averaged data. Further benefits of the real-time approach are speed of acquisition and the ability to use it during physiological interventions such as exercise or forced respiratory maneuvers.

High temporal resolution real-time imaging requires significant acceleration, beyond the level at which SENSE can produce artefact-free images. Therefore, we used UNFOLD prior to SENSE reconstruction to first halve the amount of undersampling. This was possible because each k-space position in an acquired interleave was 2× undersampled in time. Consequently, only two signal replicas centered at Nyquist and DC were present in k-f, even though the total k-space undersampling was 10×. This would also have been true if UNFOLD had been performed in x-f space, with the alternating interleave pattern similarly producing aliasing at the DC and the Nyquist frequencies (Supporting Fig. 2). Thus, irrespective of whether UNFOLD is performed in x-f or k-f space, the end result of filtering out the Nyquist temporal frequencies is halving the acceleration. In fact, UNFOLD could also have been performed in time by convolving each k/x position with the Fourier transform of the temporal frequency filter. The main reason for choosing to perform UNFOLD before SENSE was to attempt to better condition the iterative SENSE reconstruction by removing high frequency noise and improving SNR (17). However, it should be noted that this requires formal testing. When UNFOLD precedes SENSE, it is reasonable to perform UNFOLD in k-f space because no additional gridding operations are required. The main drawback is that it is not possible to use a support region technique to further improve image quality in static area of the image (6).

One important feature of our acquisition scheme was that UNFOLD was performed independently on consecutive sets of data. This had two important benefits: i) Data undergoing UNFOLD was acquired over a short period of

time (≈296 ms) compared to the respiratory period (4–6 s), which limited respiratory artefacts (18). ii) It allowed different interleaves to be acquired in each 20-frame section and enabled coil sensitivity maps to be created by combining 100 frames of data. With this self-referencing approach, coil sensitivity maps were routinely updated and provided some resilience to patient motion. It should be noted that the abrupt transitions between the 20-frame blocks undergoing UNFOLD or the 100 frame blocks undergoing SENSE could lead to temporal discontinuities. Although neither was seen in our study, methods could be employed to reduce the impact of these transitions. For instance, coil sensitivity maps could be continuously updated using a sliding window approach (this would have an impact on reconstruction time).

The rationale behind performing the UNFOLDed-SENSE reconstruction was to acquire data with high temporal resolution. The importance of temporal resolution can be appreciated by evaluating the results of the sliding window reconstructions. The SW-LFR reconstruction had the lowest temporal resolution, and this resulted in greatest blurring of the velocity curves and largest biases in the timing intervals. The SW-HTR had a higher temporal resolution than did the SW-LFR; consequently, it performed better in terms of assessment of timing intervals. However, it still did not perform as well as the UNFOLDed-SENSE reconstruction, even though the frame rate was the same. This was because of the lower effective temporal resolution, which resulted from the use of a simple box convolution kernel in the SW-HTR reconstruction.

One of the main limitations of our technique was the lack of fat suppression or water selective excitations, which can lead to image blurring at the tissue interfaces. This was not obvious in our data and may be due to the short spiral readout times. A further limitation was the significant reduction in SNR due to high levels of undersampling, although this did not affect the accuracy of the time interval assessment. Our technique could be improved by using an algebraic reconstruction (19) rather than temporal filtering. This could further improve artefact suppression, particularly ghosting due to respiratory motion.

In conclusion, we have shown that it is feasible to measure the cardiac time intervals with high temporal resolution real-time UNFOLDed-SENSE PC-MR.

ACKNOWLEDGMENTS

The authors would like to acknowledge the support received from Siemens Medical Solutions, the British Heart Foundation, and UK National Institute of Health Research (NIHR). This report is independent research by the National Institute for Health Research Biomedical Research Centre Funding Scheme. The views expressed in this publication are those of the authors and not necessarily those of the National Health Service, the NIHR, or the Department of Health.

REFERENCES

1. Oh JK, Tajik J. The return of cardiac time intervals: the phoenix is rising. J Am Coll Cardiol 2003;42:1471–1474.
2. Pruessmann KP, Weiger M, Scheidegger MB, Boesiger P. SENSE: sensitivity encoding for fast MRI. Magn Reson Med 1999;42:952–962.
3. Tsao J, Boesiger P, Pruessmann KP. k-t BLAST and k-t SENSE: dynamic MRI with high frame rate exploiting spatiotemporal correlations. Magn Reson Med 2003;50:1031–1042.
4. Hansen MS, Baltes C, Tsao J, Kozerke S, Pruessmann KP, Eggers H. k-t BLAST reconstruction from non-Cartesian k-t space sampling. Magn Reson Med 2006;55:85–91.
5. Madore B, Glover GH, Pelc NJ. Unaliasing by fourier-encoding the overlaps using the temporal dimension (UNFOLD), applied to cardiac imaging and fMRI. Magn Reson Med 1999;42:813–828.
6. Tsao J. On the UNFOLD method. Magn Reson Med 2002;47:202–207.
7. Kellman P, Epstein FH, McVeigh ER. Adaptive sensitivity encoding incorporating temporal filtering (TSENSE). Magn Reson Med 2001;45:846–852.
8. Madore B. UNFOLD-SENSE: a parallel MRI method with self-calibration and artifact suppression. Magn Reson Med 2004;52:310–320.
9. Steeden JA, Atkinson D, Taylor AM, Muthurangu V. Assessing vascular response to exercise using a combination of real-time spiral phase contrast MR and noninvasive blood pressure measurements. J Magn Reson Imaging 2010;31:997–1003.
10. Kowalik GT, Steeden JA, Pandya B, et al. Real-time flow with fast GPU reconstruction for continuous assessment of cardiac output. J Magn Reson Imaging 2012;36:1477–1482.
11. Kellman P, Sorger JM, Epstein FH, McVeigh ER. Low-latency temporal filter design for real-time MRI using UNFOLD. Magn Reson Med 2000;44:933–939.
12. Odille F, Steeden JA, Muthurangu V, Atkinson D. Automatic segmentation propagation of the aorta in real-time phase contrast MRI using nonrigid registration. J Magn Reson Imaging 2011;33:232–238.
13. Rosset A, Spadola L, Ratib O. OsiriX: an open-source software for navigating in multidimensional DICOM images. J Digit Imaging 2004;17:205–216.
14. Vivekananthan K, Kalapura T, Mehra M, et al. Usefulness of the combined index of systolic and diastolic myocardial performance to identify cardiac allograft rejection. Am J Cardiol 2002;90:517–520.
15. Nielsen JF, Nayak KS. Referenceless phase velocity mapping using balanced SSFP. Magn Reson Med 2009;61:1096–1102.
16. Steeden JA, Knight DS, Bali S, Atkinson D, Taylor AM, Muthurangu V. Self-navigated tissue phase mapping using a golden-angle spiral acquisition-proof of concept in patients with pulmonary hypertension. Magn Reson Med 2014;71:145–155.
17. Madore B. Using UNFOLD to remove artifacts in parallel imaging and in partial-Fourier imaging. Magn Reson Med 2002;48:493–501.
18. Di Bella EV, Wu YJ, Alexander AL, Parker DL, Green D, McGann CJ. Comparison of temporal filtering methods for dynamic contrast MRI myocardial perfusion studies. Magn Reson Med 2003;49:895–902.
19. Shin T, Nielsen JF, Nayak KS. Accelerating dynamic spiral MRI by algebraic reconstruction from undersampled k-t space. IEEE Trans Med Imaging 2007;26:917–924.